Efficient Computation of Physics-Compliant Channel Realizations for (Rich-Scattering) RIS-Parametrized Radio Environments

Hugo Prod'homme, Philipp del Hougne

Efficient Computation of Physics-Compliant Channel Realizations for (Rich-Scattering) RIS-Parametrized Radio Environments

Hugo Prod'homme and Philipp del Hougne, *Member, IEEE*

***Abstract*—Physics-compliant channel models for radio environments parametrized by reconfigurable intelligent surfaces (RISs) require the inversion of an "interaction matrix" to capture the mutual coupling between wireless entities (transmitters, receivers, RIS, environmental scattering objects) due to proximity *and* reverberation. The computational cost of this matrix inversion is typically dictated by the environmental scattering objects in non-trivial radio environments, and scales unfavorably with the latter's complexity. In addition, many problems of interest in wireless communications (RIS optimization, fast fading, object or user-equipment localization, etc.) require the computation of multiple channel realizations. To overcome the potentially prohibitive computational cost of using physics-compliant channel models, we *i)* introduce an isospectral reduction of the interaction matrix from the canonical basis to an equivalent reduced basis of primary wireless entities (antennas and RIS), and *ii)* leverage the fact that interaction matrices for different channel realizations only differ regarding RIS configurations and/or some wireless entities' locations.**

***Index Terms*—RIS, physics-compliant channel model, PhysFad, mutual coupling, discrete dipole approximation, scattering, isospectral reduction, inverse matrix update.**

I. Introduction

Smart radio environments in which reconfigurable intelligent surfaces (RISs) endow wireless system engineers with the ability to control the wireless channel (in addition to the usual ability to control the transmitted signals) are considered a paradigm shift that may impact future wireless network generations. However, the modeling of RIS-parametrized wireless channels is still in its infancy. Wide-spread cascaded channel models tacitly assume that multi-bounce paths can be neglected [1]. At the same time, the computational cost of existing physics-compliant models (based on polarizabilities [2] or impedances [3]–[6]) can rapidly become excessive under rich-scattering conditions [2], [6], especially if multiple channel realizations are required. The computation of multiple channel realizations is required in common problems involving RIS optimization, wireless localization and sensing, and/or fast fading, because a generic physics-compliant wireless channel depends non-linearly on the RIS configuration and/or on the location of the wireless entities [1], [7]. Here, we reduce the potentially prohibitive computational cost of evaluating multiple physics-compliant realizations of generic RIS-parametrized wireless channels by several orders of magnitude through the introduction of a reduced-basis representation of the wireless system and through efficient use of the knowledge about relations between different realizations that usually only differ regarding the RIS configuration or the locations of some wireless entities.

A RIS-parametrized wireless channel is a *linear* input-output relation that, in general, depends *non-linearly* on the RIS configuration due to *i)* proximity-induced mutual coupling between neighboring RIS elements, and *ii)* reverberation-induced long-range coupling between all RIS elements [1]. Physically, this "structural non-linearity" originates from paths involving multiple bounces between RIS elements [for *i)*] and between the RIS and other wireless entities (antennas and scattering environment) [for *ii)*] [1]. Mathematically, this "structural non-linearity" manifests itself in physics-compliant models via the inversion of an "interaction matrix" that can be cast in terms of infinite matrix power series [1]. Wide-spread cascaded models tacitly assume that these infinite series can be truncated early on such that all paths involving more than one encounter with a RIS element are neglected [1].

Recently, a polarizability-based physics-compliant end-to-end channel model for arbitrarily complex RIS-parametrized radio environments was derived from first physical principles: PhysFad [2]. Since the RIS-parametrized radio environment is a linear time-invariant[1] electrodynamical system, there must be a linear operator describing the link between the incident electromagnetic fields and the polarization fields they induce in the system. Assuming a sufficiently-high-resolution discretization of the system into polarizable elements, this operator is proportional to the inverse of an "interaction matrix"; the latter's ith diagonal entry is the inverse polarizability of the ith polarizable element and its (i,j)th off-diagonal entry is the free-space Green's function between the ith and jth polarizable elements. The polarization fields depend hence non-locally on the incident electromagnetic field because of the coupling between different polarizable elements via the non-zero off-diagonal entries of the interaction matrix. For simplicity of notation and exposition, PhysFad [2] describes each wireless entity (antenna, RIS element, scattering object) as a dipole or

P.d.H. acknowledges funding from the CNRS prématuration program (project "MetaFilt") and the ANR PRCI program (project ANR-22-CE93-0010-01).

H. Prod'homme and P. del Hougne are with Univ Rennes, CNRS, IETR - UMR 6164, F-35000, Rennes, France (e-mail: {hugo.prodhomme; philipp.del-hougne}@univ-rennes1.fr).

(Corresponding Author: Philipp del Hougne.)

[1]The RIS configuration is fixed (not time-varying) while the channel matrix is measured.

collection of dipoles.[2] The scattering response of any arbitrary anisotropic object can be equivalently described by a finite collection of fictitious dipoles [8].

Because polarizability is a local concept, the approach taken by PhysFad to describe the local changes of scattering properties as a function of the RIS configuration appears to offer the most compact formulation of a physics-compliant model. Nonetheless, equivalent formulations in terms of non-local impedances can be derived, although they tend to yield more cumbersome mathematical expressions. Prior to PhysFad, Refs. [3]–[5] already presented impedance formulations for the strongly limiting restriction of the radio environment being free space, building on an earlier proposal of a multi-port circuit theory of communications systems [9]. Very recently, Ref. [6] reproduced the PhysFad formalism in terms of impedance matrices for radio environments involving scattering objects, yielding more cumbersome mathematical expressions than PhysFad [2].

Important potential deployment scenarios of RISs at microwave and millimeter-wave frequencies, which are a significant component of sixth-generation's (6G's) all-spectra-integrated networks [10], are confronted with rich scattering within the radio environment [11]. A prototypical example is RIS-assisted machine-type communication in factories [12]. The required size of the interaction matrix to accurately describe such rich-scattering radio environments can be very large, implying a potentially prohibitively large computational cost if multiple channel realizations must be computed.

In this Letter, we alleviate this computational cost by several orders of magnitude. To this end, on the one hand, we leverage an isospectral reduction of the interaction matrix to an equivalent reduced basis of primary wireless entities (antennas and RIS). Thereby, we interpret the scattering between primary and secondary wireless entities (scattering objects) as additional coupling mechanisms between the primary wireless entities. A similar reduced-basis representation was recently used to achieve covert scattering control in metamaterials with non-locally encoded hidden symmetries [13]. On the other hand, we leverage the insight that different channel realizations typically only differ regarding some of the diagonal entries and/or some rows and columns of the interaction matrix such that updating a previously evaluated wireless channel is computationally much cheaper than evaluating it from scratch. The techniques presented in this Letter in the context of RIS-parameterized radio environments can be straightforwardly transposed to the physics-compliant modeling of dynamic metasurface antennas [14], [15].

This Letter is organized as follows. In Sec. II, we briefly review the PhysFad formalism. In Sec. III, we introduce the reduced-basis representation of PhysFad. In Sec. IV, we explain how previous channel realizations can be updated to account for a new RIS configuration (Sec. IV-A), the displacement of a wireless entity such as the user equipment or scattering objects (Sec. IV-B), or a change of the scattering objects' properties to sweep the importance of multi-path propagation (Sec. IV-C). We close with a conclusion in Sec. V.

Notation. The vector $\mathbf{a}$ containing the diagonal entries of the matrix $\mathbf{A}$ is denoted by $\mathbf{a} = \mathrm{diag}(\mathbf{A})$. $\mathbf{I}_a$ denotes the $a \times a$ identity matrix. $\left[\mathbf{A}^{-1}\right]_{\mathcal{BC}}$ denotes the block of $\mathbf{A}^{-1}$ selected by the sets of indices $\mathcal{B}$ and $\mathcal{C}$. $\delta_{i,j}$ is the Kronecker delta.

II. Generalities

Within the PhysFad framework outlined above and detailed in Ref. [2], the ith dipole, located at position $\mathbf{r}_i$, has a frequency-dependent polarizability α_i that relates the induced dipole moment p_i to the incident electromagnetic field E_i.[3] The induced dipole moment will re-radiate an electromagnetic field whose strength at the location $\mathbf{r}_j$ of the jth dipole is $G_{ji}p_i$, where G_{ji} is the free-space Green's function between positions $\mathbf{r}_i$ and $\mathbf{r}_j$. The simplest model of a RIS element is a dipole with Lorentzian polarizability whose resonance frequency is reconfigured upon changing the RIS element's configuration [2]. Thereby, the intertwinement of phase and amplitude response and their frequency selectivity are automatically captured.

Each wireless entity (antenna, RIS element, scattering object) is described as a dipole or collection of dipoles [2]. $\mathcal{N}$ denotes the set of all dipoles indices and its subsets $\mathcal{T}$, $\mathcal{R}$, $\mathcal{S}$ and $\mathcal{E}$ contain the dipole indices corresponding to the N_T transmitters, N_R receivers, N_S RIS elements, and N_E scattering objects, respectively. In total, we have $N = N_\mathrm{T} + N_\mathrm{R} + N_\mathrm{S} + N_\mathrm{E}$ dipoles. The diagonal entries of the "interaction matrix" $\mathbf{W} \in \mathbb{C}^{N\times N}$ are the dipoles' inverse polarizabilities, and the off-diagonal entries of $\mathbf{W}$ are the negatives of the corresponding Green's functions[4]:

$$W_{i,j} = \begin{cases} \alpha_i^{-1}, & i = j \\ -G_{ij}, & i \neq j \end{cases}. \tag{1}$$

We partition $\mathbf{W}$ as follows:

$$\mathbf{W} = \mathbf{W}_{\mathcal{NN}} = \begin{bmatrix} \mathbf{W}_{\mathcal{TT}} & \mathbf{W}_{\mathcal{TR}} & \mathbf{W}_{\mathcal{TS}} & \mathbf{W}_{\mathcal{TE}} \\ \mathbf{W}_{\mathcal{RT}} & \mathbf{W}_{\mathcal{RR}} & \mathbf{W}_{\mathcal{RS}} & \mathbf{W}_{\mathcal{RE}} \\ \mathbf{W}_{\mathcal{ST}} & \mathbf{W}_{\mathcal{SR}} & \mathbf{W}_{\mathcal{SS}} & \mathbf{W}_{\mathcal{SE}} \\ \mathbf{W}_{\mathcal{ET}} & \mathbf{W}_{\mathcal{ER}} & \mathbf{W}_{\mathcal{ES}} & \mathbf{W}_{\mathcal{EE}} \end{bmatrix}. \tag{2}$$

The RIS configuration $\mathbf{c} = [\alpha^{-1}_{N_\mathrm{T}+N_\mathrm{R}+1}, \ldots, \alpha^{-1}_{N_\mathrm{T}+N_\mathrm{R}+N_\mathrm{S}}] \in \mathbb{C}^{N_\mathrm{S}}$ is encoded in the $\mathbf{W}_{\mathcal{SS}}$ block: $\mathrm{diag}(\mathbf{W}_{\mathcal{SS}}) = \mathbf{c}$. The physics-compliant end-to-end channel matrix $\mathbf{H} \in \mathbb{C}^{N_\mathrm{R}\times N_\mathrm{T}}$ (assuming identical transmitting and receiving antennas for simplicity) is proportional to the $\mathcal{RT}$ block of the inverse of $\mathbf{W}$ [2]:

$$\mathbf{H} \propto [\mathbf{W}^{-1}]_{\mathcal{RT}}. \tag{3}$$

The non-linear dependence of $\mathbf{H}$ on $\mathbf{c}$ is hence apparent.

III. Reduced-Basis Representation

The wireless system engineer only has direct access to a subset of the wireless system's N internal scattering entities, namely to the $N_\mathrm{T} + N_\mathrm{R}$ antennas (for injecting and capturing waves) and the N_S RIS elements (for configuring the RIS).

[2]Extensions to multi-pole expansions of each polarizable element are conceptually straight-forward.

[3]The PhysFad framework was introduced for a 2D in Ref. [2] setting and recently experimentally validated in 3D Ref. [16].

[4]If tunable lumped circuits link specific RIS elements [17], the corresponding Green's functions are altered and to some extent controllable.

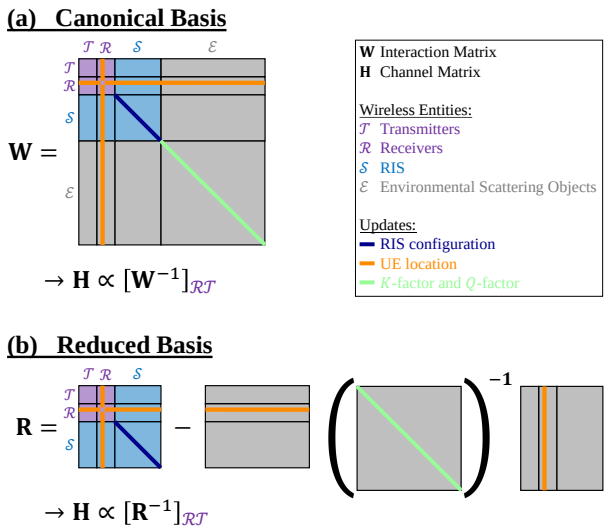

Fig. 1. Schematic illustration of a physics-compliant model's interaction matrix in the canonical (a) and reduced (b) basis. In addition, the parts of the interaction matrix affected by three types of updates are highlighted.

The set of indices of these $p = N_\mathrm{T} + N_\mathrm{R} + N_\mathrm{S}$ "primary" dipoles is $\mathcal{P} = \mathcal{T} \cup \mathcal{R} \cup \mathcal{S}$ and $\bar{\mathcal{P}} = \mathcal{N} \setminus \mathcal{P}$ contains the $s = N - p = N_\mathrm{E}$ remaining dipole indices. Hence, we seek an *equivalent* representation of the wireless system reduced to $\mathcal{P}$. We straight-forwardly rewrite $\mathbf{W}$ as a 2×2 block matrix:

$$\mathbf{W} = \begin{bmatrix} \mathbf{W}_{\mathcal{P}\mathcal{P}} & \mathbf{W}_{\mathcal{P}\bar{\mathcal{P}}} \\ \mathbf{W}_{\bar{\mathcal{P}}\mathcal{P}} & \mathbf{W}_{\bar{\mathcal{P}}\bar{\mathcal{P}}} \end{bmatrix}. \tag{4}$$

Under rich-scattering conditions, usually $p \ll s$ because many more dipoles are necessary to describe the scattering environment than to describe the antennas and the RIS. As illustrated in Fig. 1, standard formulas for the inversion of a block matrix yield

$$[\mathbf{W}^{-1}]_{\mathcal{P}\mathcal{P}} = \left(\mathbf{W}_{\mathcal{P}\mathcal{P}} - \mathbf{W}_{\mathcal{P}\bar{\mathcal{P}}}\mathbf{W}_{\bar{\mathcal{P}}\bar{\mathcal{P}}}^{-1}\mathbf{W}_{\bar{\mathcal{P}}\mathcal{P}}\right)^{-1} = \mathbf{R}^{-1} \tag{5}$$

and Eq. (3) is hence equivalent to $\mathbf{H} \propto [\mathbf{R}^{-1}]_{\mathcal{R}\mathcal{T}}$.

The dimensionality of the interaction matrix underpinning physics-compliant channel models of non-trivial RIS-parameterized radio environments involving scattering objects can hence be significantly reduced by operating in an equivalent reduced basis of primary wireless entities as opposed to the usual canonical basis. In this reduced representation, the (i,j)th off-diagonal entry of $\mathbf{R}$ accounts for coupling between the ith and jth primary dipole (antenna or RIS element) due to proximity *and* reverberation, whereas the (i,j)th off-diagonal entry of $\mathbf{W}$ only accounts for proximity-induced coupling. In addition, reverberation adds a self-coupling term such that the diagonals of $[\mathbf{W}]_{\mathcal{P}\mathcal{P}}$ and $\mathbf{R}$ differ, too. The reduced-basis representation lumps together all coupling effects between primary entities, which facilitates the calibration of the reduced-basis model (i.e., channel estimation) in an unknown rich-scattering experimental setting, as very recently achieved in Ref. [16].

IV. Computing Multiple Channel Realizations

The interaction matrices underlying different channel realizations often only differ in some details; in such cases, it is more efficient to update a previously computed channel realization than to evaluate the new channel realization from scratch. Three types of such updates of particular interest are highlighted in Fig. 1:

(i) A change in RIS configuration corresponds to a change of the diagonal of $\mathbf{W}_{\mathcal{S}\mathcal{S}}$ (highlighted in blue in Fig. 1a).

(ii) A change in the location of the ith dipole corresponds to a change of the ith row and the ith column of $\mathbf{W}$, excluding the ith diagonal entry (highlighted in orange in Fig. 1a). This case is relevant to problems in wireless localization (of a moving user equipment and/or a moving non-cooperative scattering object) as well as fast-fading scenarios (the locations of some environmental scattering objects differ across different realizations).

(iii) A change in the properties of the environmental scattering objects corresponds to a change of the diagonal of $\mathbf{W}_{\mathcal{E}\mathcal{E}}$ (highlighted in light green in Fig. 1a). Such a change is required in order to sweep the level of reverberation (quantified, e.g., by the Q-factor [18]), and it is also required in combination with (ii) to sweep through different K-factors (see Sec. III-F in Ref. [2]).

The subsequent three subsections analyze each of these three update types individually. The three update methods are mutually compatible and can hence be arbitrarily combined. In each subsection, quantities with (without) tilde denote the new (previous) channel realization. Based on the number of arithmetic operations, we consider in the following that the computational complexity is $\mathcal{O}(n_1 n_2 n_3)$ for the product of an $n_1 \times n_2$ matrix with an $n_2 \times n_3$ matrix, and $\mathcal{O}(n^3)$ for the inversion of an $n \times n$ matrix [19].

A. Updating the RIS configuration

A modification of the configuration of $m \leq N_\mathrm{S}$ RIS elements implies an update of m diagonal entries of $\mathbf{W}_{\mathcal{S}\mathcal{S}}$.[5] Knowing $\mathbf{W}^{-1}$ from the previous channel realization, the Woodbury matrix identity [20] allows us to obtain the updated inverse interaction matrix $\tilde{\mathbf{W}}^{-1}$ upon expressing the modification $\mathbf{\Delta W}$ of the interaction matrix as a product of three matrices, $\mathbf{\Delta W} = \mathbf{UCV}$,

$$\begin{aligned}\tilde{\mathbf{W}}^{-1} &= (\mathbf{W} + \mathbf{\Delta W})^{-1} = (\mathbf{W} + \mathbf{UCV})^{-1} \\ &= \mathbf{W}^{-1} - \mathbf{W}^{-1}\mathbf{U}\left(\mathbf{C}^{-1} + \mathbf{VW}^{-1}\mathbf{U}\right)^{-1}\mathbf{VW}^{-1}.\end{aligned} \tag{6}$$

Here, $\mathbf{C} \in \mathbb{C}^{m\times m}$ is a diagonal matrix containing the (by definition non-zero) changes of the inverse polarizabilities of the m modified RIS elements: $\mathrm{diag}(\mathbf{C}) = [\Delta\alpha_{n_1}^{-1}, \ldots, \Delta\alpha_{n_m}^{-1}]$, where n_k is the index of the kth modified RIS element (the modified RIS elements are not necessarily contiguous). The set of indices of the m modified dipoles is $\mathcal{M} = [n_1, \ldots, n_m]$. $\mathbf{C}$, $\mathbf{U}$ and $\mathbf{V}$ are defined as

$$[\mathbf{C}]_{k,k'} = \delta_{k,k'}\Delta\alpha_{n_k}^{-1}, \quad [\mathbf{U}]_{i,k} = [\mathbf{V}]_{k,i} = \delta_{i,n_k}. \tag{7}$$

The matrices $\mathbf{U} = \mathbf{V}^T \in \mathbb{B}^{N\times m}$ act as selectors of the indices from $\mathcal{M}$, meaning that $\mathbf{W}^{-1}\mathbf{U} = \left[\mathbf{W}^{-1}\right]_{\mathcal{N}\mathcal{M}}$, $\mathbf{VW}^{-1} = \left[\mathbf{W}^{-1}\right]_{\mathcal{M}\mathcal{N}}$, and $\mathbf{VW}^{-1}\mathbf{U} = \left[\mathbf{W}^{-1}\right]_{\mathcal{M}\mathcal{M}}$.

[5] The same method could also be applied if there was a change of the transmitting and/or receiving antennas' polarizabilities.

Since the computation of the updated channel matrix $\tilde{\mathbf{H}}$ only requires the evaluation of the $\mathcal{RT}$ block of $\tilde{\mathbf{W}}^{-1}$, the complete evaluation of $(\mathbf{W}+\mathbf{UCV})^{-1}$ in Eq. (6) is not required. Moreover, since $\mathbf{R}^{-1} \in \mathbb{C}^{p\times p}$ whereas $\mathbf{W}^{-1} \in \mathbb{C}^{N\times N}$, the cost of storing the inverse interaction matrix from the previous channel realization is lower if the discussed approach is applied not in the canonical but in the reduced basis, where $\tilde{\mathbf{R}} = \mathbf{R}+\hat{\mathbf{U}}\mathbf{C}\hat{\mathbf{V}}$ with $\hat{\mathbf{U}} = \hat{\mathbf{V}}^T = \mathbf{U}_{\mathcal{PM}} = [\mathbf{V}_{\mathcal{MP}}]^T \in \mathbb{B}^{p\times m}$. To summarize, the computationally most efficient approach to evaluate the updated channel matrix is

$$\tilde{\mathbf{H}} \propto \left[\tilde{\mathbf{R}}^{-1}\right]_{\mathcal{RT}} = \left[\left(\mathbf{R}+\hat{\mathbf{U}}\mathbf{C}\hat{\mathbf{V}}\right)^{-1}\right]_{\mathcal{RT}} = \left[\mathbf{R}^{-1}\right]_{\mathcal{RT}} - \left[\mathbf{R}^{-1}\right]_{\mathcal{RM}}\left(\mathbf{C}^{-1}+\left[\mathbf{R}^{-1}\right]_{\mathcal{MM}}\right)^{-1}\left[\mathbf{R}^{-1}\right]_{\mathcal{MT}}. \quad (8)$$

Remark: To evaluate $\tilde{\mathbf{R}}^{-1}$ instead of evaluating only $\tilde{\mathbf{H}}$, Eq. (8) can be used if both $\mathcal{R}$ and $\mathcal{T}$ are replaced by $\mathcal{P}$.

The computational complexity of Eq. (8) is $\mathcal{O}\left(m^3\right)$ for the inner matrix inversion, $\mathcal{O}\left(N_{\mathrm{R}}m^2\right)$ or $\mathcal{O}\left(N_{\mathrm{T}}m^2\right)$ for the first matrix product (depending on whether the rightmost or the leftmost is computed first), and $\mathcal{O}\left(N_{\mathrm{R}}mN_{\mathrm{T}}\right)$ for the remaining one. The computational cost can be further reduced by implementing the matrix inversion and the first matrix product as solving a system of linear equations.

This update method is referred to as method A. The resulting speed-up[6] and relative standard error (RSE) when updating $N_{\mathrm{S}} = p - N_{\mathrm{T}} - N_{\mathrm{R}}$ values of the diagonal of $\mathbf{W}_{\mathcal{PP}}$ are plotted in Fig. 2 for $N_{\mathrm{T}} = N_{\mathrm{R}} = 1$. The larger s is and the smaller p is, the more substantial speed-ups we observe, exceeding 10^3 in some cases. The RSEs are negligibly small.

In many experimental prototypes, the RIS is only 1-bit programmable (e.g., Refs. [1], [11], [16]) such that the values of the RIS dipoles' polarizabilities are limited to two values $\{\alpha_+, \alpha_-\}$. Then, two reference matrices can be computed for two complementary configurations (e.g., $\mathbf{R}_+^{-1}$ with $\alpha_i = \alpha_+ \,\forall\, i \in \mathcal{S}$ and $\mathbf{R}_-^{-1}$ with $\alpha_i = \alpha_- \,\forall\, i \in \mathcal{S}$). At update time, $m \leqq \lfloor N_{\mathrm{S}}/2 \rfloor$ can be ensured by picking the more suitable reference matrix out of $\left\{\mathbf{R}_+^{-1}, \mathbf{R}_-^{-1}\right\}$. This update method, labelled A', yields a higher speedup than A, as seen in Fig. 2, while the RSE is the same as for A.

We furthermore confirmed the accuracy of this technique by reproducing the case study on RIS-based over-the-air channel equalization for resource-constrained communications under rich scattering from Ref. [2] (Algorithm 1 and Fig. 7 therein). Using method A', Algorithm 1 from Ref. [2] converges to the same optimized configuration and yields the optimized channel impulse response (CIR) with a negligible RSE of 3×10^{-13}.

B. Updating the location of a wireless entity

A change in the location of a dipole implies that all off-diagonal entries of the corresponding row and the corresponding column of $\mathbf{W}$ are altered symmetrically. Let $\mathcal{D} = [\tilde{n}_1, \ldots, \tilde{n}_d]$ denote the set of indices of the d displaced dipoles. We use again the Woodbury identity from Eq. (6), respectively replacing $\mathbf{U}$, $\mathbf{V}$, $\mathbf{C}$ with

[6]Reported speed-ups are measured on a work station with a double Xeon E5 CPU (32 cores, 2.40 GHz) and DDR3 quad-channel memory (4×800 MHz).

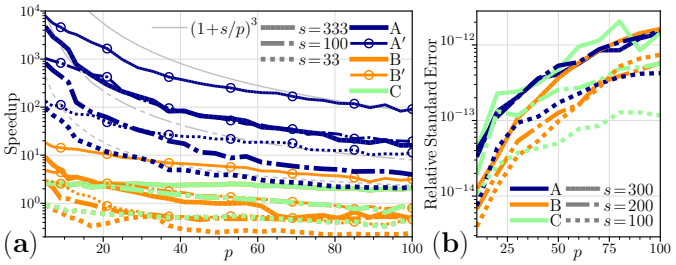

Fig. 2. (a) Speed-up (ratio of duration of full matrix inversion to duration of channel updates) and (b) RSE of the updates (full matrix inversion defines ground truth) as function of p and s for the different update methods of section IV for $N_{\mathrm{T}} = N_{\mathrm{R}} = 1$. The updated values for each method are: (A, A') $m = N_{\mathrm{S}} = p - 2$ entries of diag $(\mathbf{W}_{\mathcal{SS}})$. (B) $[(B')]$ $d = p$ rows and columns of $\mathbf{W}$ $[\mathbf{W}_{\mathcal{PP}}]$. (C) the s entries of diag $(\mathbf{W}_{\bar{\mathcal{P}}\bar{\mathcal{P}}})$.

$$\mathring{\mathbf{U}} = \left[\mathbf{K}^T \;\boldsymbol{\delta}^T\right], \quad \mathring{\mathbf{V}} = \begin{bmatrix} \boldsymbol{\delta} \\ \mathbf{K} \end{bmatrix}, \quad \mathring{\mathbf{C}} = \mathbf{I}_{2d}, \quad (9)$$

where $\mathbf{K} \in \mathbb{C}^{d\times N}$ and $\boldsymbol{\delta} \in \mathbb{B}^{d\times N}$ are defined as

$$[\mathbf{K}]_{i,j} = \begin{cases} 0, & j = \tilde{n}_i \\ \Delta G_{\tilde{n}_i,j}, & j \notin \mathcal{D} \\ \Delta G_{\tilde{n}_i,j}/2, & j \in \mathcal{D}\setminus\{\tilde{n}_i\} \end{cases}, [\boldsymbol{\delta}]_{i,j} = \delta_{\tilde{n}_i,j} \quad (10)$$

with $\Delta G_{\tilde{n}_i,j}$ being the change of the Green's function between the dipoles indexed $\tilde{n}_i$ and j. Thus, $\mathring{\mathbf{U}} \in \mathbb{C}^{N\times 2d}$ and $\mathring{\mathbf{V}} \in \mathbb{C}^{2d\times N}$, and the updated inverse interaction matrix in the reduced basis reads

$$\tilde{\mathbf{R}}^{-1} = \left[\left(\mathbf{W}+\mathring{\mathbf{U}}\mathring{\mathbf{V}}\right)^{-1}\right]_{\mathcal{PP}} = \mathbf{R}^{-1} - \left[\mathbf{W}^{-1}\right]_{\mathcal{PN}}\mathring{\mathbf{U}}\left(\mathbf{I}_{2d}+\mathring{\mathbf{U}}\mathbf{W}^{-1}\mathring{\mathbf{V}}\right)^{-1}\mathring{\mathbf{V}}\left[\mathbf{W}^{-1}\right]_{\mathcal{N}\mathcal{P}}. \quad (11)$$

A careful implementation of Eq. (11) first computes the $\mathcal{O}\left(dN^2\right)$ product $\mathbf{F} = \mathbf{K}\mathbf{W}^{-1}$ and implements the products with $\boldsymbol{\delta}$ as selection of the indices from $\mathcal{D}$:

$$\tilde{\mathbf{R}}^{-1} = \mathbf{R}^{-1} - \begin{bmatrix} \left[\mathbf{F}^T\right]_{\mathcal{PD}'} & \left[\mathbf{W}^{-1}\right]_{\mathcal{PD}} \end{bmatrix} \times \begin{bmatrix} \left[\mathbf{F}^T\right]_{\mathcal{DD}'}+\mathbf{I}_d & \left[\mathbf{W}^{-1}\right]_{\mathcal{DD}} \\ \mathbf{K}\mathbf{F}^T & \mathbf{F}_{\mathcal{D}'\mathcal{D}}+\mathbf{I}_d \end{bmatrix}^{-1} \begin{bmatrix} \left[\mathbf{W}^{-1}\right]_{\mathcal{DP}} \\ [\mathbf{F}]_{\mathcal{D}'\mathcal{P}} \end{bmatrix}, \quad (12)$$

where $\mathcal{D}' = [1, \ldots, d]$. Evaluating Eq. (12) involves an $\mathcal{O}\left(8d^3\right)$ matrix inversion, as well as two matrix products of $\mathcal{O}\left(4pd^2\right)$ and $\mathcal{O}\left(2p^2d\right)$.

Because the speedup of this update method, labelled B, chiefly depends on d, we consider the displacement of $d = p$ dipoles to display a representative speedup on Fig. 2a. When s is small (especially in comparison to p), the speedup is limited by memory access latency rather than the number of arithmetic operations, in which case the speedup can be below unity. However, we are mainly interested in cases with large s. The corresponding negligible RSEs are shown in Fig. 2b.

If all moving dipoles are primary ones (i.e., $\mathcal{D} \subset \mathcal{P}$), $\mathbf{W}_{\bar{\mathcal{P}}\bar{\mathcal{P}}}$ remains unchanged such that only $\mathbf{W}_{\mathcal{PP}}$ and $\mathbf{W}_{\mathcal{P}\bar{\mathcal{P}}} = \mathbf{W}_{\bar{\mathcal{P}}\mathcal{P}}^T$ must be updated. Using Eq. (5), evaluating $\tilde{\mathbf{R}}^{-1}$ then only requires two $\mathcal{O}\left(ps^2\right)$ and $\mathcal{O}\left(sp^2\right)$ matrix products and the $\mathcal{O}\left(p^3\right)$ matrix inversion. This method, labelled B', has a smaller memory footprint than B because it does not require full knowledge of $\mathbf{W}^{-1}$. The speedup of B' is plotted in Fig. 2(a), considering a displacement of all p primary dipoles. The

error of method B' only originates from using Eq. (5) and hence its RSE cannot exceed the one of method A. B' is faster than B overall, but requires $\mathcal{D} \subset \mathcal{P}$.

The updated $\tilde{\mathbf{R}}^{-1}$ from methods B and B' can be used directly with method A.

C. Updating the K and/or Q factor

The amount of reverberation (multi-path propagation) inside the radio environment is determined by the properties of the dipoles in $\mathcal{E}$. Changing the amount of reverberation directly alters the radio environment's Q-factor. In addition, if fast fading is implemented by moving a fixed subset of the dipoles in $\mathcal{E}$, then changing their properties will also alter the K-factor (see Sec. III-F in Ref. [2]). The ability to update the properties of the dipoles in $\mathcal{E}$ is hence essential to sweep through different types of radio environments, from free space to rich scattering. Such changes require (within the PhysFad use case considered in Sec. III-F of Ref. [2]) an identical update of the identical $s = N_{\mathrm{E}}$ diagonal entries of $\mathbf{W}_{\bar{\mathcal{P}}\bar{\mathcal{P}}} = \mathbf{W}_{\mathcal{E}\mathcal{E}}$.

To efficiently update from $\mathbf{W}^{-1}_{\bar{\mathcal{P}}\bar{\mathcal{P}}}$ to $\tilde{\mathbf{W}}^{-1}_{\bar{\mathcal{P}}\bar{\mathcal{P}}}$ upon an identical change λ of all diagonal entries of $\mathbf{W}_{\bar{\mathcal{P}}\bar{\mathcal{P}}}$, we use the eigendecomposition $\mathbf{W}_{\bar{\mathcal{P}}\bar{\mathcal{P}}} = \mathbf{Q}\mathbf{D}\mathbf{Q}^{-1}$, where $\mathbf{D}$ is a diagonal matrix whose diagonal entries are the eigenvalues of $\mathbf{W}_{\bar{\mathcal{P}}\bar{\mathcal{P}}}$ and the columns of $\mathbf{Q}$ contain the corresponding eigenvectors. Inserting $\tilde{\mathbf{W}}^{-1}_{\bar{\mathcal{P}}\bar{\mathcal{P}}} = \left(\mathbf{W}_{\bar{\mathcal{P}}\bar{\mathcal{P}}} - \lambda\mathbf{I}_s\right)^{-1} = \mathbf{Q}\left(\mathbf{D} - \lambda\mathbf{I}_s\right)^{-1}\mathbf{Q}^{-1}$ into Eq. (5) yields

$$\tilde{\mathbf{R}}^{-1} = \left(\mathbf{W}_{\mathcal{P}\mathcal{P}} - \mathbf{W}_{\mathcal{P}\bar{\mathcal{P}}}\mathbf{Q}\left(\mathbf{D} - \lambda\mathbf{I}_s\right)^{-1}\mathbf{Q}^{-1}\mathbf{W}_{\bar{\mathcal{P}}\mathcal{P}}\right)^{-1}. \quad (13)$$

The eigenvectors $\mathbf{Q}$ and $\mathbf{Q}^{-1}$ induce an important memory footprint. Hence, the most efficient evaluation of Eq. (13) consists in computing and storing the products $\mathbf{W}_{\mathcal{P}\bar{\mathcal{P}}}\mathbf{Q} \in \mathbb{C}^{p\times s}$ and $\mathbf{Q}^{-1}\mathbf{W}_{\bar{\mathcal{P}}\mathcal{P}} \in \mathbb{C}^{s\times p}$ (each with $\mathcal{O}\left(ps^2\right)$ complexity) before runtime. The inversion of the diagonal matrix $\left(\mathbf{D} - \lambda\mathbf{I}_s\right)$ only has a complexity $\mathcal{O}(s)$[7]. In addition, one of the matrix products with this diagonal matrix in Eq. (13) can be replaced with an element-wise multiplication of a row with a matrix. The last matrix product has a computational complexity of $\mathcal{O}\left(sp^2\right)$. The remaining outer matrix inversion has a computational complexity of $\mathcal{O}\left(p^3\right)$. The speedup and associated negligible RSEs of this method, labelled C, when updating the s diagonal values of $\mathbf{W}_{\bar{\mathcal{P}}\bar{\mathcal{P}}}$ are plotted in Fig. 2.

The updated $\tilde{\mathbf{R}}^{-1}$ from method C can be used directly with method A. The product $\mathbf{Q}\left(\mathbf{D} - \lambda\mathbf{I}_s\right)^{-1}\mathbf{Q}^{-1}$ provides the updated $\tilde{\mathbf{W}}^{-1}_{\bar{\mathcal{P}}\bar{\mathcal{P}}}$ that can be directly used with method B'.[8]

V. Conclusion

In order to alleviate the prohibitively large computational cost of evaluating multiple physics-compliant realizations of RIS-parametrized (rich-scattering) channels, we have introduced *i)* a reduced-basis representation of the underlying interaction matrix, and *ii)* identified efficient ways to update a previous channel realization based on how it differs from a new required realization in terms of diagonal and/or off-diagonal modifications of the underlying interaction matrix. Thereby, we enable orders-of-magnitude improvements of the computational cost of using physics-compliant models in problems involving RIS optimization, wireless localization and/or fast fading. Moreover, the proposed reduced-basis representation has recently enabled experimentally realized physics-compliant end-to-end RIS-parametrized channel estimation [16].

[7] Eq. (13) makes it easy to identify values of λ for which $\left(\mathbf{D} - \lambda\mathbf{I}_s\right)$ is ill-conditioned. In this case, which never occurred in our tests, Eq. (13) cannot be used but one could either compute the average of the channels obtained with $\lambda - \delta\lambda$ and $\lambda + \delta\lambda$, where $0 < \delta\lambda \ll \lambda$, or use the original Eq. (3).

[8] If the primary dipoles are moving through positions known in advance, the corresponding possible rows of $\mathbf{W}_{\mathcal{P}\bar{\mathcal{P}}}\mathbf{Q}$ and columns in $\mathbf{Q}^{-1}\mathbf{W}_{\bar{\mathcal{P}}\mathcal{P}}$ of Eq. (13) can be precomputed and reallocated at update time, allowing to skip the two $\mathcal{O}\left(ps^2\right)$ matrix products.

References

[1] A. Rabault *et al.*, "On the tacit linearity assumption in common cascaded models of RIS-parametrized wireless channels," *arXiv:2302.04993*, 2023.

[2] R. Faqiri *et al.*, "PhysFad: Physics-based end-to-end channel modeling of RIS-parametrized environments with adjustable fading," *IEEE Trans. Wirel. Commun.*, vol. 22, no. 1, pp. 580–595, 2023.

[3] R. J. Williams *et al.*, "A communication model for large intelligent surfaces," *Proc. ICC*, pp. 1–6, 2020.

[4] G. Gradoni and M. Di Renzo, "End-to-end mutual coupling aware communication model for reconfigurable intelligent surfaces: An electromagnetic-compliant approach based on mutual impedances," *IEEE Wirel. Commun. Lett.*, vol. 10, no. 5, pp. 938–942, 2021.

[5] S. Shen *et al.*, "Modeling and architecture design of reconfigurable intelligent surfaces using scattering parameter network analysis," *IEEE Trans. Wirel. Commun.*, vol. 21, no. 2, pp. 1229–1243, 2021.

[6] P. Mursia *et al.*, "SARIS: Scattering aware reconfigurable intelligent surface model and optimization for complex propagation channels," *IEEE Wirel. Commun. Lett.*, 2023.

[7] C. Saigre-Tardif and P. del Hougne, "Self-adaptive RISs beyond free space: Convergence of localization, sensing, and communication under rich-scattering conditions," *IEEE Wirel. Commun.*, vol. 30, no. 1, pp. 24–30, 2023.

[8] M. Bertrand *et al.*, "Global polarizability matrix method for efficient modeling of light scattering by dense ensembles of non-spherical particles in stratified media," *J. Opt. Soc. Am. A*, vol. 37, no. 1, pp. 70–83, 2020.

[9] M. T. Ivrlač and J. A. Nossek, "Toward a circuit theory of communication," *IEEE Trans. Circuits Syst. I: Regul. Pap.*, vol. 57, no. 7, pp. 1663–1683, 2010.

[10] X. You *et al.*, "Towards 6G wireless communication networks: vision, enabling technologies, and new paradigm shifts," *Sci. China Inf. Sci.*, vol. 64, no. 1, pp. 1–74, 2021.

[11] G. C. Alexandropoulos *et al.*, "Reconfigurable intelligent surfaces for rich scattering wireless communications: Recent experiments, challenges, and opportunities," *IEEE Commun. Mag.*, vol. 59, no. 6, pp. 28–34, Jun. 2021.

[12] M. Giordani *et al.*, "Toward 6G networks: Use cases and technologies," *IEEE Commun. Mag.*, vol. 58, no. 3, pp. 55–61, 2020.

[13] J. Sol *et al.*, "Covert scattering control in metamaterials with non-locally encoded hidden symmetry," *Adv. Mater.*, p. 2303891, 2023.

[14] I. Yoo *et al.*, "Analytic model of a coax-fed planar cavity-backed metasurface antenna for pattern synthesis," *IEEE Trans. Antennas Propag.*, vol. 67, no. 9, pp. 5853–5866, 2019.

[15] R. J. Williams *et al.*, "Electromagnetic based communication model for dynamic metasurface antennas," *IEEE Trans. Wirel. Commun.*, vol. 21, no. 10, pp. 8616–8630, 2022.

[16] J. Sol *et al.*, "Experimentally realized physical-model-based wave control in metasurface-programmable complex media," *arXiv:2308.02349*, 2023.

[17] H. Li *et al.*, "Beyond diagonal reconfigurable intelligent surfaces: From transmitting and reflecting modes to single-, group-, and fully-connected architectures," *IEEE Trans. Wirel. Commun.*, vol. 22, no. 4, pp. 2311–2324, 2022.

[18] J. C. West *et al.*, "Best practices in measuring the quality factor of a reverberation chamber," *IEEE Trans. Electromagn. Compat.*, vol. 60, no. 3, pp. 564–571, 2017.

[19] R. W. Farebrother, *Linear least squares computations*. Routledge, 1988.

[20] W. W. Hager, "Updating the inverse of a matrix," *SIAM Rev.*, vol. 31, no. 2, pp. 221–239, 1989.